Trends in Immunotherapy 2024, 8(2), 6825.
https://doi.org/10.24294/ti.v8.i2.6825

Article

In-silico screening of phytochemicals from *Tridax procumbens.* Linn against human neutrophil elastase targeting chronic obstructive pulmonary disease

Sudhakar Nagarajan[1], Arun D.[1], Divya Jayalakshmi K. M.[1], Prem Shankar Gupta[2], Ajay Kumar Pal[3,*], Soniya Rani[2,*]

[1] Department of Pharmacology, Sri Ramachandra Faculty of Pharmacy, Sri Ramachandra Institute of Higher Education and Research, Chennai 600-116, India
[2] Department of Pharmacology, MM College of Pharmacy, Maharishi Markandeshwar University (Deemed to be University), Ambala 133-207, India
[3] Department of Pharmacology, Delhi Pharmaceutical Sciences and Research University (DPSRU), New Delhi 110-017, India
*** Corresponding authors:** Soniya Rani, soniyapharm@gmail.com; Ajay Kumar Pal, ajaypal7894@gmail.com

CITATION

Nagarajan S, D. A, K. M. DJ, et al. In-silico screening of phytochemicals from *Tridax procumbens*. Linn against human neutrophil elastase targeting chronic obstructive pulmonary disease. Trends in Immunotherapy. 2024; 8(2): 6825. https://doi.org/10.24294/ti.v8.i2.6825

ARTICLE INFO

Received: 1 June 2024
Accepted: 11 July 2024
Available online: 2 August 2024

Abstract: With increasing environmental pollution (rising levels of air borne allergens) and smoke inhalational habits, biomass smoke, etc. all affect lung health, leading to various chronic lung diseases, and among them, life-threatening chronic obstructive pulmonary disease (COPD) is growing in prevalence around the globe. Thus, it's a great demand from researchers to discover novel therapeutic drugs and vaccines against COPD. Human neutrophil elastase (HNE) is a major inflammatory protein that triggers inflammation in chronic airway diseases, causing airway remodeling and cytokines release. Recently, it has emerged as a significant target for drug discovery in patients with COPD. Hence, this study aimed to investigate the In-silico screening of the phytochemical medicinal plant *Tridax procumbens* against COPD via targeting HNE using the Schrodinger suite 2023-1. The docking score, glide score, and binding energy were calculated by the glide program using the Prime MM-GB/SA (Molecular Mechanics with Generalized Born and Surface Area Solvation) module. The best selected phytochemicals (ligands) were then screened for pharmacokinetic properties via ADMET analysis predicted using the qikProp program. Out of the library of *Tridax procumbens*, the phytochemicals like Apigetrin, Puerarin, Centaureidin, and Myricetin significantly bind to the catalytic site of HNE with PHE41, CYS42, SER195, GLY193, PHE192, HIS57, CYS58, PHE215, SER214, ASN61, LEU998, PRO98, TYR94, and ASP95 as residues with a glide score of the highest binding affinity (−7.707, −7.707, −7.045, and −6.871, respectively) compared to the standard drugs; Dexamethasone (−4.964), Roflumilast (−4.833), and Fluticasone (−3.968). The ADMET analysis of these four phytochemicals showed good pharmacokinetic profiles with human oral absorption, log S, molar volume, and van der waals volume, etc. Thus, In-silico findings suggest that carrying out these phytochemicals (Apigetrin, Puerarin, Centaureidin, and Myricetin) from *Tridax procumbens* to validate their therapeutic potential against COPD at preclinical and clinical levels.

Keywords: ADMET; chronic obstructive pulmonary disease; human neutrophil elastase; molecular docking; MM-GBSA

1. Introduction

Chronic obstructive pulmonary disease (COPD) is a leading cause of morbidity and mortality and severe socioeconomic burden worldwide. COPD is primarily distinguished by chronic respiratory symptoms and constricted airflow. It is the third highest cause of death, with 3.23 million deaths recorded in 2019 [1]. Common symptoms of COPD include sputum development, cough, and dyspnea. Some patients with COPD experience frequent

exacerbations that aggravate respiratory symptoms and may involve lung infections or respiratory failure [2]. Smoking is the main cause of 90% of COPD cases and 80%–90% of COPD deaths. Currently, there is an FDA-approved drug for combinational therapy for COPD [3]. Airway obstruction may occasionally and partially reverse COPD. The primary factors leading to the development of COPD are exogenous oxidants such as biomass smoke, air pollution, and cigarette smoke, which cause chronic lung inflammation when inhaled [4]. The connective tissue of the lungs and airway lumen is susceptible to neutrophils and macrophages. Together, these cell types perform an essential immunological function by secreting proteases, primarily neutrophil-released elastase (HNE), proteinase 3, and macrophage-released matrix metalloprotease [5], which are intended to eliminate dead and injured cells. The production of anti-proteolytic proteins shields the lung's fragile, non-regenerative shape against proteolytic action [6]. The most significant antiproteolytic substance that neutralizes HNE is commonly referred as α1-antitrypsin. Emphysema develops as a result of increased proteolytic activity that destroys healthy lung tissue and has other roles and is thought to develop because of a shift in the protease-antiprotease balance that promotes proteolysis and causes unregulated elastase activity, which destroys the elastin lining of alveolar walls [7–10]. Plant-based flavonoids have a good pharmacological and holistic therapeutic impact against lung inflammation with minimal side effects. Therefore, this study was designed to investigate the phytochemicals of the medicinal plant *Tridax procumbens* as therapeutic molecules against HNE in COPD. Some FDA-approved drugs like Umeclidinium Bromide, Roflumilast [11], Fluticasone [12], and Dexamethasone are combinational therapies for maintaining COPD with major adverse effects, such as bladder pain, bloody nose, dribbling, and rattling breathing, etc. [13,14]. Consequently, the current research was performed In-silico molecular docking study of various phytochemicals of *Tridax procumbens* as lead molecules to determine the phytochemicals binding affinities with HNE against COPD [15].

Tridax procumbens, sometimes referred to as *Tridax Daisy* or coat buttons, is a member of the Asteraceae family. Various ailments are treated using different parts of this plant. It has a strong biological activity for curing fatal diseases because of its anti-inflammatory, immunomodulatory, anthelmintic, cardiovascular, and antiseptic properties, as well as its high propensity to repair inflammatory abnormalities [16]. Therefore, we designed the current study to evaluate the potential role of plant-based flavonoids as HNE inhibitors against COPD using In-silico methods [17,18].

This study utilized Schrodinger Suite LLC modules like Glide, Qikprop, and Prime to identify inhibitors against HNE. Additionally, MM-GBSA post-docking minimization and ADMET using Qikprop were performed to determine the physicochemical properties of phytochemicals as potential inhibitors of HNE in COPD.

2. Materials and methods

2.1. Protein preparation

The HNE protein (PDB ID: 3Q77) was retrieved from the RCSB protein data bank (https://www.rcsb.org/). The protein was preprocessed using the protein preparation wizard module of the Schrodinger suite 2023-1. The water molecules were deleted, and missing chain

atoms were added during the preprocessing step using the Schrodinger suite 2023-1 Maestro-13.5. The most stable ionization state for the heteroatom was selected. Finally, the protein structure was minimized under restricted conditions using the OPLS4 forcefield to reorient the side-chain hydroxyl groups and converge heavy atoms to an RMSD of 0.30 A^0. The active site was selected using a grid box for docking studies [19,20].

2.2. Ligand preparation

The structures of the phytochemicals were processed using the LigPrep module of Schrodinger suite 2023-1. The Epik module was used for the generation of ionization, desalting, and tautomeric states at pH of 7.0 ± 2.0. In the last step of LigPrep, phytochemicals were minimized using optimized potentials for retained specified chiralities and simulations (OPLS4) of the force field in the impact package of Schrodinger until a root mean square deviation of 1.8 A^0 was achieved. For each phytochemical, a single low-energy ring conformation was produced, and the optimized phytochemicals were utilized in docking analysis [21].

2.3. Receptor grid generation

The protein structure generated using the protein preparation wizard was used to generate the receptor lattice. To represent the centroid of the dynamic docking site, a Gride box was created. The receptor grid generation wizard is used to create a Grid box. A Grid box was generated ($x = 39.99$; $y = -12.25$; $z = -3.49$) at the centroid of the active site, keeping the Van der Waals scaling factor of 1.0 for the receptor and 0.25 as the partial charge cut-off [22].

2.4. Molecular docking studies using Glide

The phytochemicals obtained from the LigPrep module were docked using the Glide module of the Schrodinger suite 2023-1 in XP (extra precision) mode [23]. The best glide G scores for the binding modes were selected. These scores punish steric conflicts while promoting positive lipophilic, hydrogen bonding, and metal-ligand interactions. The results of the docking studies were analyzed using the glide module's XP visualizer [24]. The glide scores of the molecules were compared with those of commonly used standard COPD medications, such as Roflumilast, Fluticasone, Dexamethasone, and Umeclidinium Bromide. Docking factors like lipophilic perseverance, in which the ligands are completely enclosed in the lipophilic pocket, are mostly responsible for the glide scoring capacity. The binding affinity can be increased by other factors, such as electrostatic forces and hydrogen bonds with ligands. The glide score can be reduced by some unfavorable factors, such as XP and rotational penalties, etc. [19].

2.5. ADMET profile

The Qikprop module based on the Schrodinger suite 2023-1 was implemented to determine the ADMET profile of the phytochemicals. Prediction of physically and pharmacokinetically significant descriptors for the predicted properties like molecular weight, hydrogen bond acceptor, donor count, log P, total solvent accessible surface area, No. of

violations in Lipinski's Rule of Five, human oral absorption, log S, molar volume, and van der waals volume etc. [20].

2.6. Binding free energy calculation using the prime/MM-GBSA approach

The binding free energy of phytochemicals was calculated using the Prime MM-GB/SA module of Schrodinger suite 2023-1. The OPLS4 force field was used to minimize energy for the XP docked pose of the ligand receptor complex, and the Generalized Born/Surface Area (GB/SA) band VSGB 2.0 (Variable-dielectric Surface Generalized Born) solvent mode was used to estimate the solvation free energy of a molecule in a given solvent [25,26]. Prime MMGBSA DG bind, the binding free energy was calculated using the equation:

$$\Delta G \text{ (bind)} = \text{E complex (minimized)} + \text{E receptor (minimized)} - \text{E ligand (minimized)} \quad (1)$$

3. Results and discussion

The affinity of the phytochemicals (A1–A28) with HNE is described in **Table 1** in terms of XP docking and glide scores. The docking studies of the phytochemicals and HNE were conducted using the XP docking program with the Glide module of the Schrodinger suite 2023-1 Maestro-13.5. The designed phytochemicals were docked with HNE to assess their COPD inhibitory activity. A root mean square difference (RMSD) of 0.2 for the molecules indicates the best fit. The phytochemical's docking scores were in the range from −7.707 to −2.327 (**Table 1**). PHE41, CYS42, SER195, GLY193, PHE192, HIS57, CYS58, PHE215, SER214, ASN61, LEU998, PRO 98, TYR94, and ASP95 are the active residues of HNE involved in the binding of the ligands. Aigetrin has the highest XP docking score of −7.707, followed by the phytochemicals Puerarin, Centauredin, and Myricetin (−7.693, −7.045, and −6.871, respectively) **Figure 1A–H**. The standard drugs, including Dexamethasone, Roflumilast, and Fluticasone exhibited docking scores of −4.964, −4.833, and −3.968 with HNE, respectively **Figure 2A–F**. These phytochemicals demonstrate pi-pi stacking with HIS57 and form hydrogen bonds with PHE41, SER195, and GLY193 residues. These docked phytochemicals also showed excellent dock scores compared with the standard drugs Dexamethasone, Roflumilast, and Fluticasone. Additionally, molecular docking was assessed with MMGBSA free restricting vitality, which was identified using the post-scoring approach for COPD targeting HNE. The values are described in **Table 2**. All of the proposed analogues showed good free binding energies, which suggests that they fit well into the HNE receptor. The binding free energy of Apigetrin exhibited the highest ΔG binding energy (59.3 kcal/mol) with HNE.

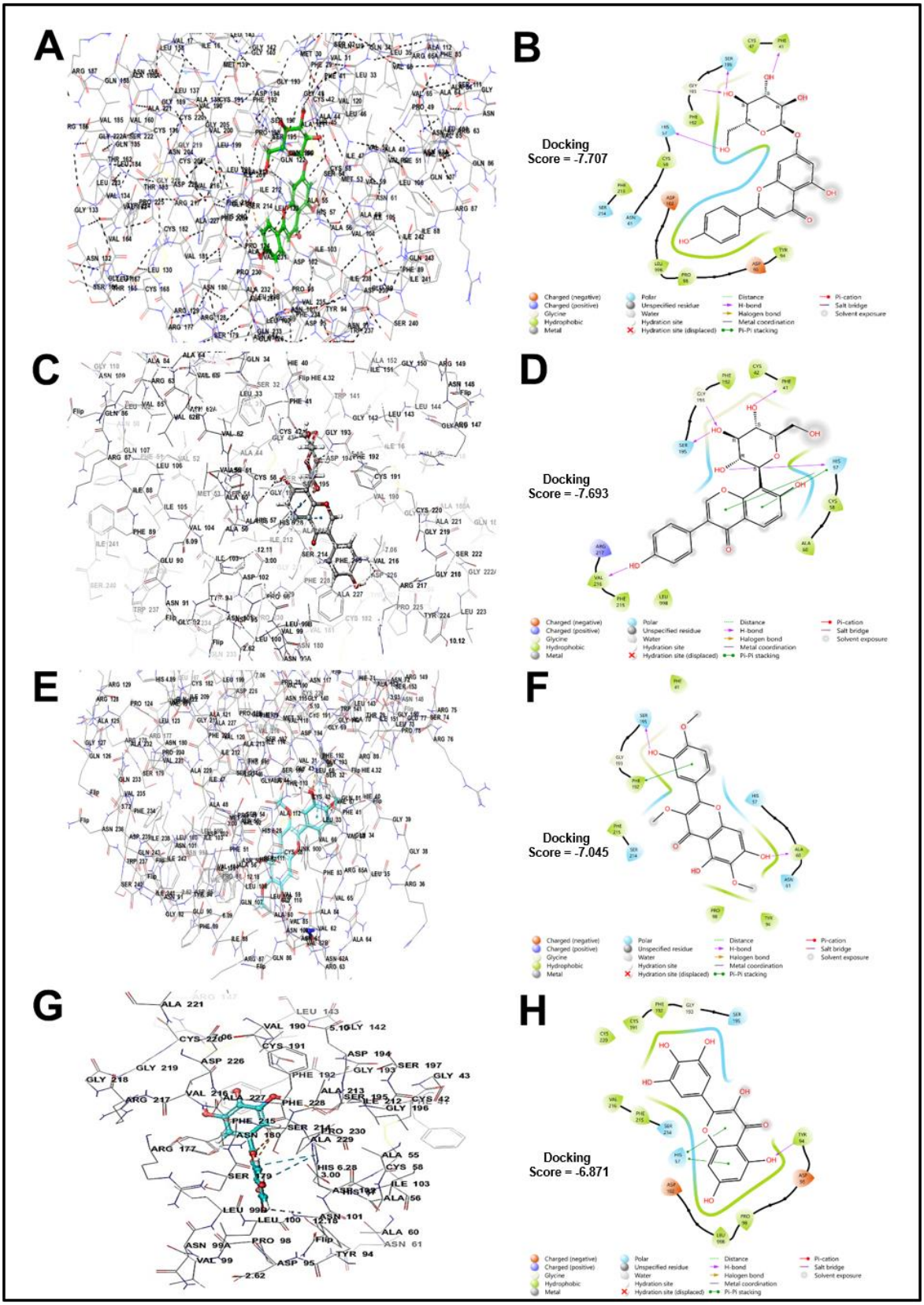

Figure 1. 2D and 3D representation of docking complex of Apigetrin (A1), Puerarin (A2), Centaureidin (A3), and Myricetin (A4) with Human neutrophil elastase (HNE). 3D representation of **(A)** Apigetrin; **(C)** Puerarin; **(E)** Centataureidin; and **(G)** Myricetin with HNE complex. 2D representation of **(B)** Apigetrin; **(D)** Puerarin; **(F)** Centataureidin; and **(H)** Myricetin with HNE complex.

Table 1. The tabular representationof docking results of In-silico screening of phytochemicals from *Tridax procumbens* based on their XP docking scores against Human neutrophil elastase (HNE) target (PDB ID: 3Q77).

ID	Phytochemicals	XP docking score	XP glide score	Glide score	Glide emodel
A1	Apigetrin	−7.707	−7.707	−7.707	−57.357
A2	Puerarin	−7.693	−7.703	−7.703	−53.878
A3	Centaureidin	−7.045	−7.083	−7.083	−46.597
A4	Myricetin	−6.871	−6.917	−6.917	−50.153
A5	Robinetin	−6.271	−6.316	−6.316	−48.933
A6	Nodakenin	−6.186	−6.186	−6.186	−48.301
A7	Bergenin	−6.054	−6.084	−6.084	−41.728
A8	Quercetin	−6.007	−6.047	−6.047	−48.179
A9	Kaempferol	−5.284	−5.323	−5.323	−42.781
A10	Luteolin	−4.995	−5.043	−5.043	−43.708
A11	Dexamethasone	−4.964	−4.964	−4.964	−39.716
A12	Biochanin A	−4.875	−4.905	−4.905	−37.567
A13	Roflumilast	−4.833	−4.833	−4.833	−49.41
A14	Apigenin	−4.812	−4.86	−4.86	−42.441
A15	Naringenin	−4.792	−4.816	−4.816	−41.823
A16	Daidzein	−4.762	−4.773	−4.773	−30.865
A17	Budesonide	−4.728	−4.728	−4.728	−48.921
A18	Genistein	−4.374	−4.404	−4.404	−37.624
A19	Beta-Sitosterol	−4.344	−4.344	−4.344	−28.709
A20	Umeclidinium bromide	−4.296	−4.296	−4.296	−63.957
A21	Fluticasone	−3.968	−3.968	−3.968	−43.604
A22	Nobiletin	−3.873	−3.873	−3.873	−21.23
A23	Indacaterol	−3.683	−3.735	−3.735	−52.917
A24	Lupeol	−3.05	−3.05	−3.05	−30.906
A25	Limonene	−3.038	−3.038	−3.038	−21.795
A26	β-Stigmasterol	−2.377	−2.377	−2.377	−26.254
A27	Caryophyllene	−2.342	−2.342	−2.342	−18.435
A28	Taraxasterol acetate	−2.327	−2.327	−2.327	−37.959

Table 2. Tabular representation of binding free energy calculation using Prime/MM-GBSA approach of phytochemicals (A1–A28) from *Tridax procumbens*.

ID	Compounds	Prime energy	MMGBSA dG Bind	MMGBSA dG Bind Coulomb	MMGBSA dG Bind Covalent	MMGBSA dG Bind Hbond
A1	Apigetrin	−8751.9	−59.3	−28.15	6.9	−2.85
A2	Puerarin	−8658.9	−47.93	−35.5	5.87	−3.32
A3	Centaureidin	−8673	−48.37	−34.91	4.56	−2.1
A4	Myricetin	−8736.3	−47.93	−21.13	2.94	−1.31
A5	Robinetin	−8628.4	−38.13	−13.94	5.11	−1.55

Table 2. (*Continued*).

ID	Compounds	Prime energy	MMGBSA dG Bind	MMGBSA dG Bind Coulomb	MMGBSA dG Bind Covalent	MMGBSA dG Bind Hbond
A6	Nodakenin	−8511.6	−59.04	−14.36	2.91	−2.22
A7	Bergenin	−8451.4	−37.81	−26.79	3.54	−1.88
A8	Quercetin	−8720	−34.6	−12.23	2.28	−1.47
A9	Kaempferol	−8725.8	−28.86	−11.11	1.35	−0.98
A10	Luteolin	−8803.4	−32.57	−13.18	1.21	−1.21
A11	Dexamethasone	−8441	−47.66	−23.12	1.18	−1.54
A12	Biochanin A	−8777	−31.42	−17.31	1.56	−1.07
A13	Roflumilast	−8499	−49.6	−7.61	0.16	−0.81
A14	Apigenin	−8816.4	−29.21	−11.63	0.85	−1.09
A15	Naringenin	−8692.9	−38.03	−5.09	0.74	−0.62
A16	Daidzein	−8692.6	−30.63	−18.67	3.15	−1.1
A17	Budesonide	−8495.9	−42.47	−14.44	7.94	−1.26
A18	Genistein	−8789.1	−35.86	−15.15	2.69	−1.59
A19	Beta−Sitosterol	−8497.5	−30.51	−15.59	8.58	−1.02
A20	Umeclidinium Bromide	−8470.4	−58.32	47.1	7.72	−0.21
A21	Fluticasone	−8454.8	−36.41	−13.58	7.39	−1.07
A22	Nobiletin	−8571.1	−33.16	0.56	4.79	−0.49
A23	Indacaterol	−8539.6	−43.5	35.08	2.23	−1.19
A24	Lupeol	−8458.1	−32.02	−14.13	0.46	−0.98
A25	Limonene	−8511.6	−28	0.8	1.47	0
A26	Stigmasterol	−8510.5	−35.48	−8.49	1.05	−0.51
A27	Caryophyllene	−8496.8	−22.71	1.36	0.79	0
A28	Taraxasterol acetate	−8464.4	−34.99	−6.12	2.14	−0.47

To establish the interactions of phytochemicals (A1–A28) with HNE, molecular docking studies assessments were carried out (**Figure 1** and **2, Table 1**) implementing molecular docking techniques, and the binding mechanisms of the phytochemicals were examined. The docking and glide scores of docking studies against HNE are presented in **Table 1**, and the results were compared with those obtained using standard drugs.

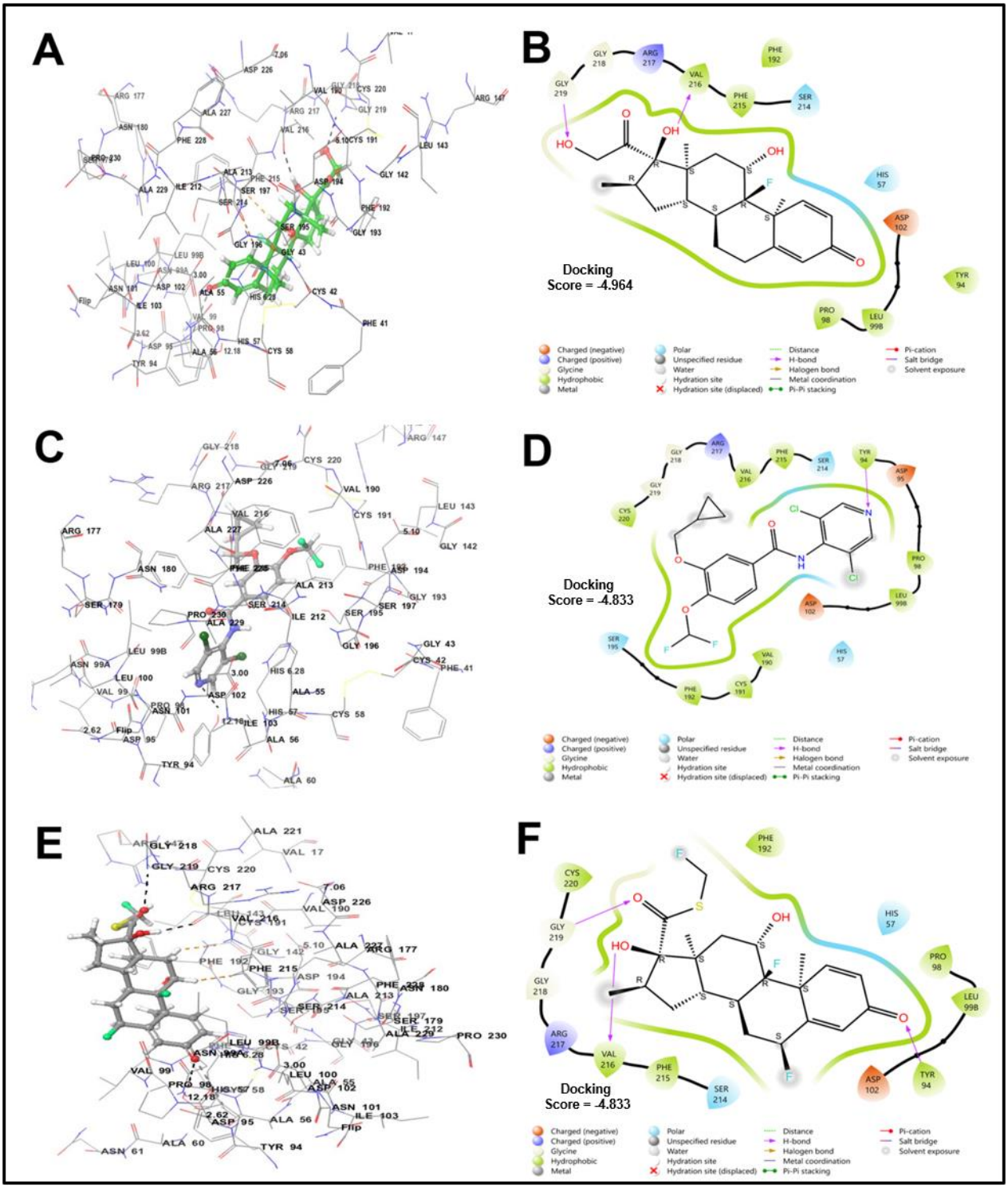

Figure 2. 2D and 3D representation of docking complex of Dexamethasone (A11), Roflumilast (A13), and Fluticasone (A21) with Human neutrophil elastase (HNE). 3D representation of **(A)** Dexamethasone; (**C**) Roflumilast; and (**E**) Fluticasone with HNE complex. (**B**) 2D representation of Dexamethasone; (**D**) Roflumilast; and (**F**) Fluticasone with HNE complex.

According to Lipinski's Rule of Five, a molecule should have a molecular weight of ≤500, A Rule of 5, and the number of hydrogen bond donors and acceptors should be 0.0 to 06 and 2.0 to 20.0, respectively. These characteristics have been identified as important for

determining oral bioavailability and molecular flexibility. As a result, the ability of the phytochemicals to follow this rule was assessed, and all of the generated phytochemicals followed Lipinski's Rule of Five. According to In-silico ADMET screening, most of the designed phytochemicals follow the recommended ranges (**Table 3**). Prime MM-GSBA

Table 3. In-silico prediction of ADMET profile of phytochemicals from *Tridax procumbens* and standard drugs.

Phytochemicals	mol MW[a]	Donor HB[b]	Accept HB[c]	QPlogP o/w[d]	QPlog herg[e]	Rule of five[f]	Human oral absorption[g]
Nodakenin	408.404	4	12.5	−0.066	−5.084	0	2
Lupeol	426.724	1	1.7	7.055	−3.494	1	1
Limonene	136.236	0	0	3.981	−3.262	0	3
Caryophyllene	204.355	0	0	5.037	−2.881	1	3
Bergenin	328.275	5	12.05	−1.564	−3.707	0	2
Apigetrin	432.383	5	12.25	−0.311	−5.998	1	2
Centaureidin	360.32	2	6	2.175	−4.629	0	3
Beta-Sitosterol	414.713	1	1.7	7.393	−4.421	1	1
Stigmasterol	412.698	1	1.7	7.396	−4.467	1	1
Taraxasterol acetate	468.762	0	2	7.862	−4.224	1	1
Puerarin	416.384	6	12.5	−0.534	−5.965	1	2
Robinetin	302.24	5	6.25	−0.181	−5.045	0	2
Biochanin A	284.268	1	3.75	2.516	−5.051	0	3
Myricetin	318.239	5	6	−0.303	−4.932	1	2
Nobiletin	402.4	0	7	3.733	−4.946	0	3
Genistein	270.241	2	3.75	1.694	−5.042	0	3
Daidzein	254.242	2	4	1.792	−5.152	0	3
Naringenin	272.257	2	4	1.549	−4.73	0	3
Kaempferol	286.24	3	4.5	1.036	−5.14	0	3
Apigenin	270.241	2	3.75	1.624	−5.125	0	3
Luteolin	286.24	3	4.5	0.941	−5.022	0	3
Quercetin	302.24	4	5.25	0.362	−5.035	0	2
Roflumilast	403.212	1	4.75	4.845	−5.332	0	3
Indacaterol	392.497	4	6.45	2.622	−6.623	0	2
Fluticasone	444.508	2	6.45	3.693	−4.188	0	3
Budesonide	430.54	2	9.85	2.128	−4.242	0	3
Dexamethasone	392.466	3	8.15	1.827	−3.873	0	3

[a]Molecular weight, Da (range for phytochemicals: 136–468 Da).
[b]Predicted number of hydrogen bonds that would be donated by the solute to water molecules in an aqueous solution.
[c]Predicted number of hydrogen bonds that would be accepted by the solute from water molecules in an aqueous solution.
[d]Predicted octanol/water partition coefficient.
[e]Predicted IC50 value for blockage of HERG k+ channels.
[f]Number of violations of Lipinski's rule of five.
[g]Predicted human oral absorption.

analysis shows the relative binding energies of each phytochemical to the HRE. It results from several ligand protein interactions, including polar, hydrophobic, covalent, and other interactions. Due to the high negative values generated by all phytochemicals, the MM-GBSA assay results revealed that the energies that strongly bind ligands in the binding pocket of HNE are Van der Waals energy (GvdW) and non-polar solvation (GLipo). Other energies, such as electrostatic solvation energy (GSolv) and covalent energy (GCov), do not significantly encourage receptor binding. Additionally, higher values of GVdW and GLipo in the negative range demonstrate a noteworthy hydrophobic interaction with HNE and phytochemicals A1–A28. The phytochemicals A1-4, A11, A13, and A20 showed highly preferred ligand binding. Since compound A1-4 had the greatest docking score and indicated its prime energy ranged from 8441 to 8816.4 kcal mol^{-1}, the finding is also linked to the docking and glide scores. A vital component in the interaction between drugs and receptors, examining the lowest energy poses predicted by the scoring function demonstrates the accuracy of docking. By docking ligands into the coupling pocket, the docking score, glide score, and MM-GBSA free energy are obtained, and the phytochemicals are more stable.

4. Conclusions

Based on the docking results, the phytochemicals of *Tridax procumbens* were better arranged at a dynamic site. The In-silico approach used in this study was essential for identifying certain phytochemicals and may also aid in clarifying their usefulness for future investigations like in-vitro and in-vivo experiments. The results of the In-silico investigation revealed that many phytochemicals of *Tridax procumbens* may be therapeutically more effective against COPD by inhibiting HNE. Based on In-silico studies, *Tridax procumbens* phytochemicals like Apigetrin, Puerarin, Centaureidin, and Myricetin are significantly active and have better pharmacological activity against inflammation by inhibiting HNE with potential therapeutic benefits. Thus, they are likely to be useful after further development. In conclusion, the phytochemicals A1–A10 exhibited therapeutic efficacy and were identified as potential molecules. *Tridax procumbens* based phytochemicals in the form of medicines may therefore be an effective treatment option for COPD.

Author contributions: Conceptualization, SR, AKP and PSG; methodology, SN; software, SN; validation, SN, SR and AKP; formal analysis, SN and SR; investigation, SN; resources, SN and SR; data curation, SN, AD and DJKM; writing—original draft preparation, SN; writing—review and editing, SR and AKP; visualization, SN and SR; supervision, SR and AKP; project administration, SR. All authors have read and agreed to the published version of the manuscript.

Acknowledgments: The authors sincerely thank Sri Ramachandra Faculty of Pharmacy, Sri Ramachandra Institute of Higher Education and Research, Chennai for providing the necessary facilities required to conduct this research. The authors would also like to thank Maharishi Markendeshwar Deemed to be University, Haryana for providing other necessary facilities.

Conflict of interest: The authors declare no conflict of interest.

Abbreviations

HNE	Human neutrophil elastase
ADMET	Absorption distribution metabolism excretion and toxicity
TP	*Tridax procumbens*
MM−GBSA	Molecular mechanics/Generalized born surface area
PDB	Protein data bank
XP	Extra precision
MW	Molecular weight
ΔG bind	Free energy of binding
COPD	Chronic obstructive pulmonary disease

References

1. Singh D, Agusti A, Anzueto A, et al. Global Strategy for the Diagnosis, Management, and Prevention of Chronic Obstructive Lung Disease: the GOLD science committee report 2019. European Respiratory Journal. 2019; 53(5): 1900164. doi: 10.1183/13993003.00164-2019
2. Zhang MY, Jiang YX, Yang YC, et al. Cigarette smoke extract induces pyroptosis in human bronchial epithelial cells through the ROS/NLRP3/caspase-1 pathway. Life Sciences. 2021; 269: 119090. doi: 10.1016/j.lfs.2021.119090
3. Hansen G, Gielen-Haertwig H, Reinemer P, et al. Unexpected Active-Site Flexibility in the Structure of Human Neutrophil Elastase in Complex with a New Dihydropyrimidone Inhibitor. Journal of Molecular Biology. 2011; 409(5): 681-691. doi: 10.1016/j.jmb.2011.04.047
4. Abboud RT, Vimalanathan S. Pathogenesis of COPD. Part I. The role of protease-antiprotease imbalance in emphysema, 2008.
5. Kulkarni T, O'Reilly P, Antony VB, et al. Matrix Remodeling in Pulmonary Fibrosis and Emphysema. American Journal of Respiratory Cell and Molecular Biology. 2016; 54(6): 751-760. doi: 10.1165/rcmb.2015-0166ps
6. Gadek JE, Fells GA, Zimmerman RL, et al. Antielastases of the human alveolar structures. Implications for the protease-antiprotease theory of emphysema. Journal of Clinical Investigation. 1981; 68(4): 889-898. doi: 10.1172/jci110344
7. Wang Z, Chen F, Zhai R, et al. Plasma Neutrophil Elastase and Elafin Imbalance Is Associated with Acute Respiratory Distress Syndrome (ARDS) Development. PLoS ONE. 2009; 4(2): e4380. doi: 10.1371/journal.pone.0004380
8. Voynow J, Fischer B, Zheng S. Proteases and cystic fibrosis. The International Journal of Biochemistry & Cell Biology. 2008; 40(6-7): 1238-1245. doi: 10.1016/j.biocel.2008.03.003
9. Hofman PM. Pathobiology of the neutrophil-intestinal epithelial cell interaction: Role in carcinogenesis. World Journal of Gastroenterology. 2010; 16(46): 5790. doi: 10.3748/wjg.v16.i46.5790
10. Inoue Y, Omodani T, Shiratake R, et al. Development of a highly water-soluble peptide-based human neutrophil elastase inhibitor; AE-3763 for treatment of acute organ injury. Bioorganic & Medicinal Chemistry. 2009; 17(21): 7477-7486. doi: 10.1016/j.bmc.2009.09.020
11. Wang C, Zhou J, Wang J, et al. Progress in the mechanism and targeted drug therapy for COPD. Signal Transduction and Targeted Therapy. 2020; 5(1). doi: 10.1038/s41392-020-00345-x
12. Yip E, Karimi S, T. Pien L. Evaluation of a Therapeutic Interchange from Fluticasone/Salmeterol to Mometasone/Formoterol in Patients with Chronic Obstructive Pulmonary Disease. Journal of Managed Care & Specialty Pharmacy. 2016; 22(4): 316-323. doi: 10.18553/jmcp.2016.22.4.316
13. Babu KS, Morjaria JB. Umeclidinium in chronic obstructive pulmonary disease: latest evidence and place in therapy. Therapeutic Advances in Chronic Disease. 2017; 8(4-5): 81-91. doi: 10.1177/2040622317700822
14. Quint JK, Ariel A, Barnes PJ. Rational use of inhaled corticosteroids for the treatment of COPD. npj Primary Care Respiratory Medicine. 2023; 33(1). doi: 10.1038/s41533-023-00347-6

15. Chaudhari HC, Patil KP, Mandal PSGVP. A Review on Medicinal Importance of Tridax Procumbens Linn. Research & Reviews in Pharmacy and Pharmaceutical Sciences. 2022.
16. Ingole VV, Mhaske PC, Katade SR. Phytochemistry and pharmacological aspects of Tridax procumbens (L.): A systematic and comprehensive review. Phytomedicine Plus. 2022; 2(1): 100199. doi: 10.1016/j.phyplu.2021.100199
17. Kalirajan R, Muralidharan V, Jubie S, et al. Microwave assisted synthesis, characterization and evaluation for their antimicrobial activities of some novel pyrazole substituted 9-anilino acridine derivatives. International Journal of Health & Allied Sciences. 2013; 2(2): 81. doi: 10.4103/2278-344x.115682
18. Grace VMB, Viswanathan S, Wilson DD, et al. Significant action of Tridax procumbens L. leaf extract on reducing the TNF-α and COX-2 gene expressions in induced inflammation site in Swiss albino mice. Inflammopharmacology. 2019; 28(4): 929-938. doi: 10.1007/s10787-019-00634-0
19. Gálvez J, Polo S, Insuasty B, et al. Design, facile synthesis, and evaluation of novel spiro- and pyrazolo[1,5-c]quinazolines as cholinesterase inhibitors: Molecular docking and MM/GBSA studies. Computational Biology and Chemistry. 2018; 74: 218-229. doi: 10.1016/j.compbiolchem.2018.03.001
20. Rani S, Ansari MN, Saeedan AS, Kaithwas G . Novel Quinazoline Derivative Activates FIH-1 in MCF-7 Cells and 7, 12-Dimethylbenz[a]-Anthracene Induced Mammary Gland Carcinoma in Albino Rats. J Biol Regul Homeost Agents. 2024; 38(5). doi: 10.23812/j.biol.regul.homeost.agents.20243805.330
21. Kalirajan R, Muralidharan V, Jubie S, et al. Synthesis of Some Novel Pyrazole-Substituted 9-Anilinoacridine Derivatives and Evaluation for their Antioxidant and Cytotoxic Activities. Journal of Heterocyclic Chemistry. 2012; 49(4): 748-754. doi: 10.1002/jhet.848
22. Roos K, Wu C, Damm W, et al. OPLS3e: Extending Force Field Coverage for Drug-Like Small Molecules. Journal of Chemical Theory and Computation. 2019; 15(3): 1863-1874. doi: 10.1021/acs.jctc.8b01026
23. Jacobson MP, Pincus DL, Rapp CS, et al. A hierarchical approach to all-atom protein loop prediction. Proteins: Structure, Function, and Bioinformatics. 2004; 55(2): 351-367. doi: 10.1002/prot.10613
24. Barros RO, Junior FLCC, Pereira WS, et al. Interaction of Drug Candidates with Various SARS-CoV-2 Receptors: An in Silico Study to Combat COVID-19. Journal of Proteome Research. 2020; 19(11): 4567-4575. doi: 10.1021/acs.jproteome.0c00327
25. Naresh P, Selvaraj A, Shyam SP, et al. Targeting a conserved pocket (n-octyl-β-D-glucoside) on the dengue virus envelope protein by small bioactive molecule inhibitors. Journal of Biomolecular Structure and Dynamics. 2020; 40(11): 4866-4878. doi: 10.1080/07391102.2020.1862707
26. Li J, Abel R, Zhu K, et al. The VSGB 2.0 model: A next generation energy model for high resolution protein structure modeling. Proteins: Structure, Function, and Bioinformatics. 2011; 79(10): 2794-2812. doi: 10.1002/prot.23106